UC Riverside

UC Riverside Previously Published Works

Title

Optical trapping in the presence of laser-induced thermal effects.

Permalink

https://escholarship.org/uc/item/5qk5v9qq

Journal

Optics Letters, 45(14)

ISSN

0146-9592

Authors

Zenteno-Hernandez, JA
Vázquez Lozano, J
Sarabia-Alonso, JA
et al.

Publication Date

2020-07-15

DOI

10.1364/ol.394647

Copyright Information

This work is made available under the terms of a Creative Commons Attribution License, available at https://creativecommons.org/licenses/by/4.0/

Peer reviewed

eScholarship.org Powered by the California Digital Library
University of California

Optics Letters

Optical trapping in the presence of laser-induced thermal effects

J. A. Zenteno-Hernandez, J. Vázquez Lozano,* J. A. Sarabia-Alonso, J. Ramírez-Ramírez, and R. Ramos-García

Departamento de Óptica, Instituto Nacional de Astrofísica, Óptica y Electrónica, Luis Enrique Erro #1, Tonantzintla, Puebla 72840, Mexico
**Corresponding author: jvazquez@inaoep.mx*

Received 7 April 2020; revised 4 June 2020; accepted 5 June 2020; posted 9 June 2020 (Doc. ID 394647); published 10 July 2020

The inclusion of thermal effects in optical manipulation has been explored in diverse experiments, increasing the possibilities for applications in diverse areas. In this Letter, the results of combined optical and thermal manipulation in the vicinity of a highly absorbent hydrogenated amorphous silicon layer, which induces both the generation of convective currents and thermophoresis, are presented. In combination with the optical forces, thermal forces help reduce the optical power required to trap and manipulate micrometric polystyrene beads. Moreover, the inclusion of these effects allows the stacking and manipulation of multiple particles with a single optical trap along with the beam propagation, providing an extra tool for micromanipulation of a variety of samples. © 2020 Optical Society of America

https://doi.org/10.1364/OL.394647

The number of applications of optical manipulation has increased drastically since being discovered by Ashkin *et al*. [1]. To measure the stiffness of an optical trap, several techniques have been proposed [2], such as the drag force method [3], the power spectrum density method [4], and the equipartition method [5]. The equipartition method, or the Boltzmann statistic method, shows excellent results when working with smaller particles and weak optical traps but is unreliable at high optical powers because of the increased Brownian motion due to heating [6]. The power spectrum method offers high precision in the measurements of small forces but a higher sensitivity to temperature variations [6]. Finally, the method based on viscous drag force, despite requiring the most information of the experiment to be measured and most post-processing effort, offers the most accurate stiffness values for studies involving large displacements of the sample from the trapping spot. Moreover, this method is an excellent option in the absence of a quadrant detector and the use of known diameter spherical microparticles [7].

Thermal effects may affect the optical trapping performance due to the increased thermal energy of the particles [8]. In addition, it may damage biological samples, therefore, absorption is generally avoided in optical trapping experiments. Nevertheless, it has been proved that thermal effects may provide new tools for optical manipulation of different types of particles in an aqueous media [9]. Thermal effects have shown advantages over optical and electric systems, owing to their low power requirements and simple experimental setups, allowing the manipulation of multiple particles at temperatures that do not represent a threat to the sample. Many of these experiments rely on heat-induced convective currents, where an induced temperature gradient in the sample cell creates a flow in the liquid from the hot zones to the cold ones, thus gathering particles around the heating zone. Moreover, convective currents have been used to collect and sort particles that are not necessarily close to the trapping spot [10,11]. It has been demonstrated that these convective currents allow thermal manipulation of microparticles [12], DNA [13], and even single nanoparticle trapping [14].

In this Letter, we propose a technique to increase the stiffness of an optical trapping system with the inclusion of thermal effects, specifically convective currents, and thermophoresis. This is done by depositing a thin film of hydrogenated amorphous silicon (a-Si:H) on one of the chamber's walls that locally heats the sample up upon illumination. Using low optical powers, an equilibrium between optical forces and thermal forces is achieved. The resulting stiffness coefficient of the trap is then measured through the drag force method. Comparing the trapping stiffness in samples with and without the thin absorbing layer lets us differentiate the contribution of each optical and thermal phenomenon.

Experiments were carried out using two kinds of chambers: one using bare glass coverslips (no thermal effects) and another with a 1 μm thick a-Si:H film deposited on one of the coverslips, as depicted in Fig. 1. The chamber was filled with a colloidal mixture of polystyrene microparticles with a 1.5 μm radius immersed in water. An unexpanded laser emitting at 532 nm, always focused 10 μm above the thin layer with a 100× oil-immersion objective (Edmund Optics) was used to trap the particles.

Light absorption at the a-Si:H film ($\alpha_{a\text{-Si}} \sim 2.77 \times 10^4\ \mathrm{cm}^{-1}$ at $\lambda = 532$ nm) produces a temperature gradient ∇T that heats the water up according to the heat transfer equation, where a steady-state condition is assumed, given by Eq. (1) [10]:

$$\rho c_p u \cdot \nabla T = \nabla \cdot (K \nabla T) + Q, \tag{1}$$

where ρ is the water density, c_p is its heat capacity, u is the fluid's field velocity field, K is the thermal conductivity, and $Q = \alpha I_0$

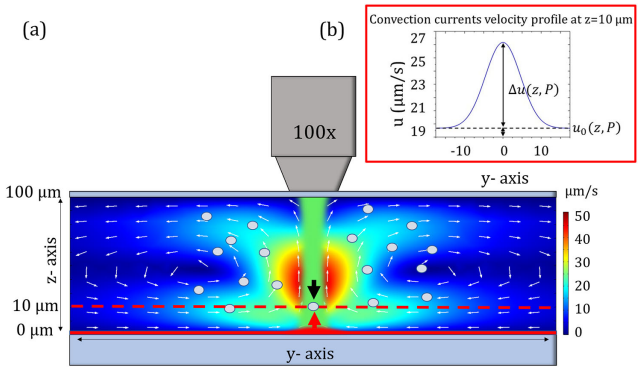

Fig. 1. (a) Schematic representation of the 1.5 μm polystyrene particles (gray circles) inside the chamber under the presence of convective currents (white arrows) generated by the thermal gradient induced by light absorption at the a-Si:H film (red line at the bottom of the sample cell). The scattering force exerted on the particle (indicated by the black arrow directed downward) is partially compensated by the longitudinal gradient force, the convective currents, and the thermophoretic force at $z = 10$ μm with an optical power of $P = 3$ mW. The red zone near the center of the sample cell indicates the area of the highest convective liquid speed obtained with COMSOL Multiphysics (figure not in scale). (b) Transversal convective currents velocity Gaussian type profile at $z = 10$ μm. The maximal temperature at $z = 10$ μm reached in our experiments was $T = 305$ K, according to the simulation.

is the heat source per volume unit, with α as the absorption coefficient and I_0 as the intensity of the optical source. In addition, pressure work and viscous heating are not considered. Amorphous silicon is treated as the only heat source because its absorption coefficient is much higher than the one of water [10].

In order to model the convective currents, the Navier-Stokes equations for incompressible flow, Eqs. (2) and (3), were solved [10] together with the heat transfer equation using COMSOL Multiphysics:

$$\rho\,(u\cdot\nabla)\,u = \nabla\cdot\left\{-pI + \mu\left[\nabla u + (\nabla u)^T\right]\right\} + F_b, \tag{2}$$

$$\rho\nabla\cdot u = 0, \tag{3}$$

where a Gaussian beam is incident (along the z axis, as shown in Fig. 1) on the absorbing film heating the adjacent layer and setting in motion the convective currents, p is the pressure of the fluid, μ is the dynamic viscosity of the fluid, and I is the 2nd order identity tensor. The driving mechanism is the buoyancy force per unit volume of the fluid F_b defined as $F_b = g(\rho - \rho_0)$, where ρ and ρ_0 are the water's densities after the laser has been turned on and at room temperature, respectively. The coupling between these equations leads to convective currents in a closed chamber (100×250 μm^2), as shown in Fig. 1. The convective currents are directed upward, just above the hot spot (where the laser is incident), reach the upper surface, move parallel to the upper substrate away from the center and then direct toward the vertical walls, and finally, at the lower substrate, move parallel to the substrate toward the hot spot. Near the center of the chamber, the speed reaches its highest value.

Once the particle was trapped, the chamber was displaced perpendicularly to the beam propagation direction using a computer-controlled translation stage (Model NanoMax-TS 381 by Thorlabs). This displacement Δy allows the measurement of the maximum speed of the particle before escaping the trap. Since the particles were trapped close to the substrate ($z \sim 10$ μm), the Faxen correction to the drag force F_d felt by a sphere was considered [5]. This correction depends on the distance z of the trapped object from the bottom of the chamber to the particle of radius R. The value of F_d experienced by the particle is given by [15] as

$$F_d = 6\pi R\mu' u = 6\pi R\upsilon\frac{\mu}{1 - \frac{9}{16}\left(\frac{R}{z}\right) + \frac{1}{8}\left(\frac{R}{z}\right)^3 - \frac{45}{256}\left(\frac{R}{z}\right)^4 - \frac{1}{16}\left(\frac{R}{z}\right)^5}, \tag{4}$$

where υ is the velocity of the translation stage or the particle in the experiment. For this specific case of $z = 10$ μm, F_d has a variation of 9%, compared to the case when the correction was not considered. The trapped particle was displaced a distance Δy from its equilibrium position when the chamber was displaced at a constant drag speed υ, so

$$6\pi R\mu'\upsilon = k\Delta y, \tag{5}$$

where $R = 1.5$ μm and k (N/m) is the trap stiffness. Then, the displacement Δy can be expressed as the product of the velocity υ times a constant value β as shown in Eq. (6):

$$\Delta y = \left(\frac{6\pi\mu' R}{k}\right)\upsilon = \beta\upsilon. \tag{6}$$

Since the values of the $\mu_{\text{water }298\text{ K}} = 8.91 \times 10^{-4}$ N · s/m^2 (bare glass), $\mu_{\text{water }305\text{ K}} = 7.81 \times 10^{-4}$ N · s/m^2 (absorbing film), Δy, and the velocity υ were known, k could be determined. A typical plot of velocity against displacement obtained from Eq. (6), is shown in Fig. 2 (in this case, for a cell with bear glass).

Therefore, the stiffness coefficient k can be obtained from the slope β of the linear fitting shown in Fig. 2; as the speed was increased, the trapped particle eventually escapes out of the trap

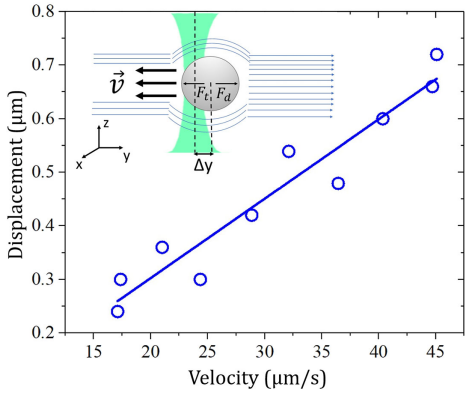

Fig. 2. Representation of the viscous drag force method for measuring the stiffness of a conventional optical trap without a-Si:H. The displacement of the cell at constant speed displaces the microparticle from its equilibrium position by a distance Δy. In this new equilibrium position, two forces interact with the particle: the optical trapping force F_t and the transversal drag force F_d. For a polystyrene particle of $R = 1.5$ μm, 10 μm above the a-Si:H film, and a power of $P = 4.5$ mW with $\beta = 0.0145$ s, a stiffness value of $k \approx 1.9$ pN/μm was obtained.

at a critical speed (<45 μm/s at $P = 4.5$ mW with bare cover glass for Fig. 2).

The trap stiffness k was measured for different laser powers in both chambers when the particle was trapped at $z \sim 10$ μm above the bottom coverslip. The results for both cases are shown in Fig. 3. One can observe that the stiffness for the chamber with the a-Si:H layer can be up to ∼3 times larger than the chamber with no absorbing film, depending on the optical power. Also, the trapped particle in the heated cell can be dragged at higher velocities, i.e., with a power of 3 mW in the heated cell, the measured velocity was $\upsilon \sim 90$ μm/s, while with the bare layer, the velocity was 3 times smaller ($\upsilon \sim 30$ μm/s) (See Visualization 1).

Moreover, the trapping threshold decreases thanks to the presence of the thermal effects, in this case, from 2 mW down to 1 mW. Optical powers >3.5 mW were not used when absorbing substrates were present because they can give rise to vapor bubbles or even cavitation-bubbles if higher powers are used. Maximal temperatures reached with 3 mW were around $T = 305$ K at $z = 10$ μm. However, one can extend the operating range of the traps by carefully controlling the heat source intensity, which depends on the absorption coefficient, the thickness of the thin a-Si:H layer, the location of the focal plane, and the size of the beam spot.

To understand the increase in the stiffness of the trap, special attention should be paid to the forces associated with convective currents and to thermophoretic effects associated with temperature gradients. From the COMSOL simulations displayed in Fig. 1(b), a Gaussian profile of the fluid velocity perpendicular to the beam propagation was found to have a form of the type:

$$u(r, z, P) = u_0(z, P) + \Delta u(z, P) \exp\left[-\left(\frac{r}{2r_0(z)}\right)^2\right], \tag{7}$$

where P is the optical power, $u_0(z, P)$ is the offset velocity, $\Delta u(z, P)$ is the difference between the maximum velocity and the offset velocity, r is the radial coordinate, and $r_0(z, P)$ is the characteristic distance. The change in coordinates is a consequence of the symmetry of the problem. To keep consistency with the experiment, the focal plane was located at $z = 10$ μm above the thin film with an optical power of $P = 3.5$ mW.

Similar flow profiles were obtained due to light absorption in bulk water when NIR radiation was used in optical trapping experiments [16]. It was shown that strong absorption in water can thermally induce a localized flow, which exerts an additional velocity gradient force on the particles that complements the optical gradient force [16].

Figure 4(a) shows the transversal velocity gradient for different distances z from the a-Si:H film. Figure 4(b) shows the associated trapping potential for both the transversal optical forces and the one associated with the fluid velocity profile at $z = 10$ μm, calculated from the linear region of the optical gradient and velocity gradient. To estimate the optical potential without thermal effects, a Matlab code reported in Ref. [17] was used, and its results were validated using the optical toolbox developed by Nieminem *et al.* [18], simulating a Gaussian beam with a waist around ∼3 μm, 3.5 mW optical power, and 1.5 μm radius particles. Since there is no analytical expression for the fluid velocity potential, it was not possible to calculate the actual value, and only its spatial dependence is represented in Fig. 4(b). It is clear that the optical potential (blue) is more localized in the transversal direction r than the one associated with thermal fluid velocity potential. When the particle is laterally displaced at a given speed, it may escape from the optical potential but will stay inside the thermal one and remain trapped, this might explain the results observed in Fig. 3.

In the experiment, it was noteworthy that the trapped particles might become out of focus depending on the trapping position within the chamber (pushed in the opposite direction of the beam propagation). There may be two reasons for the defocusing of the particle: the force associated with convective currents and the thermophoretic force. The convection currents force F_{cc} will be proportional to the velocity of the fluid along the upper direction for $r = 0$ against the beam propagation. The thermophoretic force F_{Tp} arises by the temperature gradient ∇T due to light absorption at the a-Si:H film. However, it is extremely difficult to measure and calculate it since no analytical solutions exist for liquids [12]. What is known is that particles around a temperature gradient may be expelled or attracted from the hot region depending on the sign of the particle's thermophoretic diffusion coefficient D_T. The particle's thermophoretic velocity is given by $u_{th} = -D_T \nabla T$ [19]. The temperature profile extracted from the COMSOL simulation under the conditions previously mentioned decreases exponentially along the propagation distance z as

$$T(z, r = O) = T_{RT} + \Delta T\left[\exp\left(-\frac{z}{z_D}\right)\right], \tag{8}$$

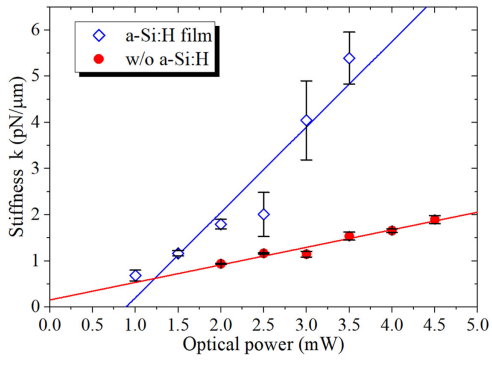

Fig. 3. Values of the trap stiffness as a function of the optical power with and without thermal effects measured at a distance $z \sim 10$ μm from the bottom of the cell for $R = 1.5$ μm radius particles.

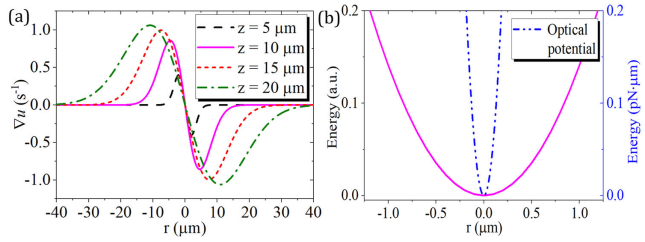

Fig. 4. (a) Velocity gradient perpendicular to the direction of propagation z at different positions along the z axis. (b) Potential wells are obtained from the linear region of the velocity gradients. In blue, the optical potential well; in pink, the potential well associated with convective currents at $z = 10$ μm. It is evident that the stiffness of the trap increases because of the additional potential well associated with the temperature. When a particle frees itself from the optical trap, the thermal potential keeps it in place.

where $T_{RT} = 298.6$ K, $\Delta T = 78.4$ K, and the heat diffusion length $z_D = 4.1$ μm. From this expression, it was possible to obtain the temperature gradient. Just to give an estimate of the order of magnitude of the thermophoretic velocity, we take a value $D_T = 10$ μm^2/K [11,19], reported for a 1.5 μm particle's radius, with $\nabla T = -1.68 \times 10^6$ K/m, located at the focal plane $z = 10$ μm above the substrate, the thermophoretic velocity has a value around $u_{th} \sim 16.9$ μm/s in the upper direction, which is comparable, at this position, with the velocity related to convective currents $u(z = 10\ \mu m)$. The associated thermophoretic force must depend on this velocity, but an analytical expression cannot be written as pointed out above. This force sets a new equilibrium position for the trapped particle determined by the superposition of the longitudinal gradient force F_{opt}, the scattering force F_{scat}, the force associated with convection currents F_{cc}, and the thermophoretic force F_{Tp}. Finding the new equilibrium position is not easy, since the calculation of optical forces in the presence of thermal effects is a rather complicated problem. To the best of our knowledge, there is no model that can tackle this issue. To change this position, $F_{Tp} + F_{cc}$ must be of the order of $F_{scat} + F_{opt}$. In the experiment, the larger the contribution of $F_{Tp} + F_{cc}$, the larger the defocusing of the trapped particle.

For regions located $z < 10$ μm above the substrate, F_{Tp} dominates over the optical forces and may displace the particles from the equilibrium position of the trap. For regions located $z > 20$ μm above the substrate, F_{cc} increases its value and pushes the particles away from the trapping zone reaching velocities up to ∼50 μm/s. The region located in the range between 10 μm and 20 μm above the a-Si:H thin layer, offers a region where the trapped particle is more or less in focus.

In fact, we found experimentally that in this region, manipulation and trapping of multiple particles along the z axis are possible, which was not observed in the chamber with no absorbing film (See Fig. 5). In Visualization 2, particles around the beam (hot region) were dragged to the trap by convective currents, and some of them might enter the trapping region from below pushing up (and defocusing) the already trapped particle.

Our experimental results showed that up to 4 particles were trapped along the z axis. Even when different groups report manipulation of several particles due to thermal effects [11,19], this is the first time that multiple stacked particles trapping and manipulation with one single focused beam combining both thermal and optical forces with a relatively simple experimental setup is achieved to the best of our knowledge. This increases the possibilities of the system reported here to manipulate multiple objects with low optical powers (∼3.5 mW).

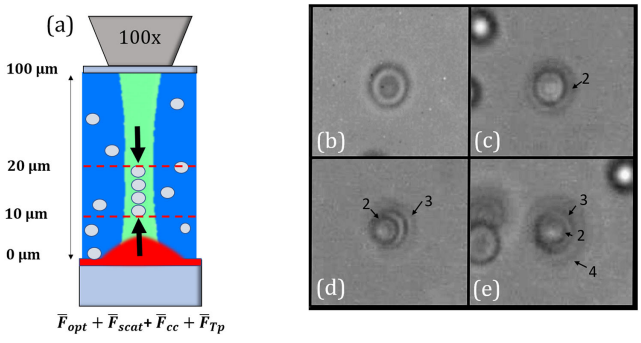

Fig. 5. (a) Schematic representation (not in scale) of the chamber and experimental observation of the multiple particles trapped under the same trap. Experimental image sequence on the right shows consecutive trapping and defocusing of the four particles transported into the trap by convective currents. (b) Zoomed single trapped particle. (c) Two trapped particles. (d) Three trapped particles. (e) Four trapped particles and their silhouette. It is evident that the previously trapped particles defocus when a new particle enters the trap. (see Visualization 2).

In conclusion, we demonstrated the enhancement of the trap stiffness (spring constant) of an optical trap with particles suspended in water by laser-induced thermal convective currents and thermophoresis. These effects are the result of thermal gradients created by light absorption in a thin layer of a-Si:H deposited at the bottom of the chamber, where the microparticles are suspended. The trap stiffness was enhanced up to a factor ∼3 when convective currents and thermophoretic forces were present. A trapped particle can be dragged (by moving the translation stage perpendicular to the propagating axis) at velocities as high as 90 μm/s without escaping the trap, whereas with no a-Si:H film, the particle escapes at lower velocities (30 μm/s). Thermal effects open the possibility of massive trapping of microparticles at power as low as 1 mW with a single laser spot, specifically for applications where the sample is extremely sensible either to optical power or absorption.

Funding. Fondo de Cooperación Internacional en Ciencia y Tecnología (C0013-2014-01-246648).

Disclosures. The authors declare no conflicts of interest.

REFERENCES

1. A. Ashkin, Phys. Rev. Lett. **24**, 156 (1970).
2. N. Malagnino, G. Pesce, A. Sasso, and E. Arimondo, Opt. Commun. **214**, 15 (2003).
3. M. C. Williams, in *Single Molecule Techniques* (2002), pp. 1–14.
4. L. P. Ghislain, N. A. Switz, and W. W. Webb, Rev. Sci. Instrum. **65**, 2762 (1994).
5. H. Felgner, O. Müller, and M. Schliwa, Appl. Opt. **34**, 977 (1995).
6. M. Sarshar, W. T. Wong, and B. Anvari, J. Biomed. Opt. **19**, 115001 (2014).
7. S. F. Tolić-Nørrelykke, E. Schäffer, J. Howard, F. S. Pavone, F. Jülicher, and H. Flyvbjerg, Rev. Sci. Instrum. **77**, 103101 (2006).
8. P. Kumari, J. A. Dharmadhikari, A. K. Dharmadhikari, H. Basu, S. Sharma, and D. Mathur, Opt. Express **20**, 4645 (2012).
9. G. Liu and J. C. Giddings, Chromatographia **34**, 483 (1992).
10. E. Flores-Flores, S. A. Torres-Hurtado, R. Páez, U. Ruiz, G. Beltrán Pérez, S. L. Neale, J. C. Ramírez-San-Juan, and R. Ramos-García, Biomed. Opt. Express **6**, 4079 (2015).
11. S. Duhr and D. Braun, Phys. Rev. Lett. **97**, 1 (2006).
12. M. Braun, T. Thalheim, K. Günther, M. Mertig, and F. Cichos, Proc. SPIE **9922**, 99220Z (2016).
13. D. Braun and A. Libchaber, Phys. Rev. Lett. **89**, 188103 (2002).
14. M. Braun and F. Cichos, ACS Nano **7**, 11200 (2013).
15. C. N. Davies, *Low Reynolds Number Hydrodynamics, with Special Applications to Particulate Media* (2003), Vol. **6**.
16. Y. Liu and A. W. Poon, Opt. Express **18**, 18483 (2010).
17. J. G. Ortega-Mendoza, F. Chávez, P. Zaca-Morán, C. Felipe, G. F. Pérez-Sánchez, G. Beltran-Pérez, O. Goiz, and R. Ramos-García, Opt. Express **21**, 6509 (2013).
18. T. A. Nieminen, N. R. Heckenberg, and H. Rubinsztein-Dunlop, Proc. SPIE **5514**, 514 (2004).
19. S. Duhr and D. Braun, Phys. Rev. Lett. **96**, 168301 (2006).

192.168.172.174 [ts: 2020-07-09 12:30:31]